ELSEVIER

Progress in Nuclear Magnetic Resonance Spectroscopy 45 (2004) 301–313

PROGRESS IN NUCLEAR MAGNETIC RESONANCE SPECTROSCOPY

www.elsevier.com/locate/pnmrs

Spin counting

Colan E. Hughes

Department of NMR Based Structural Biology, Max Planck Institute for Biophysical Chemistry, Am Faßberg 11, 37077 Göttingen, Germany

Received 30 June 2004

Contents

Keywords: Spin counting; Multiple-quantum coherences; Gaussian and non-Gaussian distributions; Liquid crystals; Dimensionality; Quadrupolar nuclei; Amyloid fibrils

1. Introduction

Spin counting is the name given to a group of nuclear magnetic resonance (NMR) experiments which assess the number of nuclear spins present in an interacting network. The direct correlation to *atom* counting means that spin counting presents a method by which NMR can establish molecular forms and interactions, although rarely in a manner from which detailed structural information can be independently obtained. The somewhat qualitative nature of

E-mail address: hugh@nmr.mpibpc.mpg.de

doi:10.1016/j.pnmrs.2004.08.002

Nomenclature

$c_{zz}^{(i,j)}$, $c_{\pm}^{(i,j)}$, $c_{+}^{(i,j)}$	coefficients for the $I_z^{(i)}I_z^{(j)}$, $I_+^{(i)}I_-^{(j)}$, $I_+^{(i)}I_+^{(j)}$ Hamiltonian terms
$\mathcal{H}_{0Q}$	Hamiltonian containing terms which do not change the coherence order
$\mathcal{H}_{1Q}$	Hamiltonian containing terms which change the coherence order by ± 1
$\mathcal{H}_{2Q}$	Hamiltonian containing terms which change the coherence order by ± 2
I	spin quantum number
$I_x^{(i)}$, $I_y^{(i)}$, $I_z^{(i)}$	spin operators for spin i
$I_+^{(i)}$, $I_-^{(i)}$	raising and lowering operators for spin i
$\mathcal{I}(p)$	intensity of p-quantum filtered signal
n	number of spins involved in a given magnetization state
m_c, m_t	pre-exponential factors in a two-Gaussian model for the signal intensities
N	number of spins in a cluster
N_t, N_c	coefficients in a two-Gaussian model for the signal intensities
p	coherence order of a given magnetization state
$p^{(y)}$	coherence order with respect to the y-axis
s	time domain signal
z	any integer
z_g	any even integer
z_u	any odd integer
$Z(p)$	number of p-quantum states in a given spin system
$\Delta\phi$	increment in the phase of a pulse
τ	duration of a delay
ϕ	phase of a pulse
χ	flip angle of a pulse
ADRF	adiabatic demagnetization in the rotating frame
ARRF	adiabatic remagnetization in the rotating frame
fpRFDR	finite pulse radio frequency driven recoupling
REDOR	rotational echo double resonance
RFDR	radio frequency driven recoupling
SEDOR	spin echo double resonance

many spin counting results might imply that such methods are only of limited use in a research community equipped with an array of methods for measuring internuclear distances and other structural restraints. Nevertheless, spin counting has been implemented in a number of cases to provide highly important, fundamental structural information.

The origins of spin counting lie in solution-state experiments, where J-coupling networks can be examined, leading to conclusions regarding molecular connectivity [1]. This has since been augmented with solid-state applications, in which spatial proximity is probed via dipolar interactions [2,3]. It is these solid-state applications which will form the bulk of the material covered by this review. Most spin counting methods rely upon the observation of multiple-quantum coherences and much effort has been spent developing and assessing multiple-quantum excitation schemes within the context of spin counting, along with developing methods for the efficient observation of multiple-quantum coherences. One other important aspect of spin counting is the method by which the results should be interpreted.

This review will examine the basic principles of spin counting, looking at the different ways in which it has been carried out, as dictated by the nature of the samples being studied. One section will examine the various multiple-quantum excitation methods, with a view to identifying the advantages and disadvantages of the various classes. Another section is devoted to the analysis of spin counting results, examining the means by which a seemingly simple result has been treated. Finally, a review of the various applications of spin counting is given.

The name spin counting is also given to experiments which make an analytical measurement of the relative concentrations of particular nuclear species in a sample, particularly samples of natural organic matter such as soils. These experiments are not the subject of this review and readers are directed to Refs. [4,5] and references therein.

2. Basic principles

A magnetization state of multiple-quantum coherence with order $\pm p$ in a system of nuclei with spin I is indicative of the presence of at least $p/(2I)$ spins in a coupled network. Thus, by establishing what is the maximum possible multiple-quantum coherence order that can be excited, a count of the number of spins in a coupled network may be made. However, because the excitation of a magnetization state of multiple-quantum coherence with order $\pm p$ does not exclude the presence of more than $p/(2I)$ spins, such a count can only be considered to place a *minimum bound* on the number of spins present, unless it may be established that higher coherence orders cannot be excited and are not absent purely due to experimental deficiencies or restrictions.

It is often the goal of spin counting experiments to excite and observe a state of total coherence [6], in which the coherence order is the maximum allowed for the coupled

spin network. Such states have unique properties among all the possible magnetization states, properties which may be exploited to verify their presence [7,8] (see Section 4.3). However, spin counting may also be applied to differentiate between small, isolated spin systems and extended networks of spins. In the latter case, total coherence may be unattainable but the observation of very high coherence orders will still carry important information. Furthermore, systems with known extended networks can also be studied using spin counting, as the speed of build up of multiple-spin states will depend upon the nature of the network, such as the dimensionality.

Most spin counting experiments rely upon the correlation between the coherence order of the state and the minimum number of spins that must be involved in the state. However, magnetization states can involve more spins than their coherence order demands. Consider, for example, states such as $I_z^{(i)}I_z^{(j)}$ and $I_+^{(i)}I_-^{(j)}$, both two-spin states with zero coherence order. By changing the quantization axis against which the coherence order is measured (i.e. switching from the z-axis to the x- or y-axis), multiple-spin states which do not have a coherence order relative to the z-axis which is indicative of the number of spins present can be used for spin counting [9] (see Section 3.6).

Of particular importance in solution-state studies are experiments which make use of multiple-quantum filtration to simplify and analyse spectra of complex molecules [10,11]. These methods rely upon the same basic principle as spin counting, namely that a p-quantum magnetization state can only come from a spin system of at least $p/(2I)$ interacting nuclei. This has been used to filter for the signal from specific molecular moieties [12].

3. Experimental methods

3.1. Multiple-quantum filters

The basis of most spin counting techniques is a filtration experiment, consisting of an excitation sequence and a reconversion sequence between which a multiple-spin state exists. With the exception of methods utilising dipolar order (see Section 3.6), the experiments are multiple-quantum filters. Three generic sequences are shown in Fig. 1. They differ in the way in which hard 90° r.f. pulses are combined with periods during which zero-quantum (0Q), single-quantum (1Q) or double-quantum (2Q) Hamiltonians are applied. Other possible sequences are, of course, possible, such as those which commence with cross-polarization rather than a simple 90° pulse.

The classification of Hamiltonians as zero-quantum, single-quantum or double-quantum indicates the change in coherence order between the states of magnetization they interconvert. For a system of spins $I=1/2$, a typical

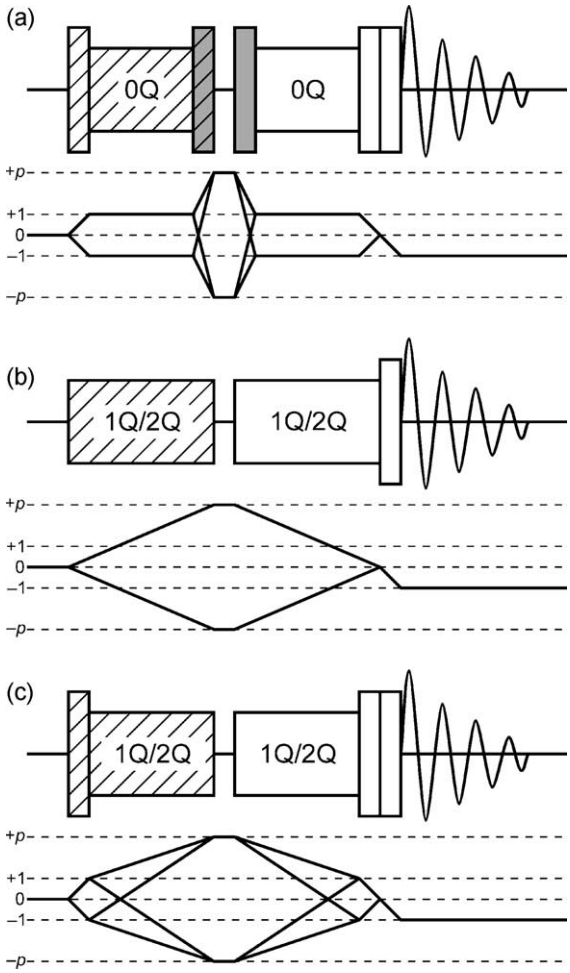

Fig. 1. Schematics of spin counting experiments. The taller rectangles indicate 90° pulses. (a) A zero-quantum scheme, in which transverse magnetization evolves under a zero-quantum operator to generate anti-phase magnetization from which multiple-quantum states may be excited. The phases of the shaded 90° pulses are chosen to select particular parities of the coherence order. (b) A spin counting experiment commencing from longitudinal magnetization, using single- or double-quantum operators to directly excite multiple-quantum states. (c) A spin counting experiment commencing from transverse magnetization, using single- or double-quantum operators to excite multiple-quantum states. In all three experiments, the hatching indicates those parts of the pulse sequence to which a phase, ϕ, is applied. This phase can be cycled to achieve multiple-quantum filtering or incremented to generate a single data set showing all excited coherence orders.

zero-quantum Hamiltonian would have the general form

$$\mathcal{H}_{0Q} = \sum_{i>j} c_{zz}^{(i,j)} I_z^{(i)} I_z^{(j)} + c_{\pm}^{(i,j)} I_+^{(i)} I_-^{(j)} + c_{\pm}^{(i,j)*} I_-^{(i)} I_+^{(j)}, \quad (1)$$

where the sum is over spin pairs (i, j). A single-quantum Hamiltonian will have a form such as

$$\mathcal{H}_{1Q} = \sum_{i>j} c_{xz}^{(i,j)} I_x^{(i)} I_z^{(j)} + c_{zx}^{(i,j)} I_z^{(i)} I_x^{(j)}, \quad (2)$$

whilst a double-quantum Hamiltonian will have the general form

$$\mathcal{H}_{2Q} = \sum_{i>j} c_{+}^{(i,j)} I_{+}^{(i)} I_{+}^{(j)} + c_{+}^{(i,j)*} I_{-}^{(i)} I_{-}^{(j)}. \quad (3)$$

The terms $c_{zz}^{(i,j)}$, $c_{\pm}^{(i,j)}$, $c_{xz}^{(i,j)}$, $c_{zx}^{(i,j)}$ and $c_{+}^{(i,j)}$ will be functions of the various nuclear interactions, with the through-bond J-coupling and the through-space dipolar coupling being the most significant.

All the individual terms shown above involve two-spins. Such terms will induce transitions between magnetization states which increase or decrease the number of spins involved in the state by one. Most multiple-quantum excitation sequences make use of Hamiltonians consisting of such two-spin terms but operators involving more spins can also be exploited in multiple-quantum filtration experiments [13,14]. For quadrupolar nuclei ($I > 1/2$), there will also be one-spin, multiple-quantum terms present in the Hamiltonian, resulting from the quadrupolar interaction [15]. These terms will induce changes in coherence order without changing the number of spins involved in the magnetization state.

Fig. 1a shows the use of a zero-quantum Hamiltonian, bracketed between two 90° pulses, to excite multiple-quantum coherences. A similar sequence is used to reconvert the multiple-quantum coherences to observable single-quantum coherences [7]. A zero-quantum Hamiltonian cannot cause a change in the coherence order of the magnetization state. Consequently, the zero-quantum Hamiltonian is applied to a state of transverse magnetization (created by the first 90° pulse), transforming in-phase terms such as $I_x^{(i)}$ into anti-phase terms such as $I_y^{(i)} I_z^{(j)}$, from which multiple-quantum coherences may be excited by the second 90° pulse. The phases of the two 90° pulses before and after the filtration point (shaded grey in Fig. 1a) determine the parity of the coherence orders which are excited and observed (see Section 3.2).

Fig. 1b shows the use of a single- or double-quantum Hamiltonian to excite multiple-quantum coherence from Zeeman magnetization. The reconversion proceeds in two steps; first a single- or double-quantum Hamiltonian is applied to generate Zeeman magnetization, then a 90° pulse generates observable single-quantum coherences. In this case, the single- or double-quantum Hamiltonian can directly excite multiple-quantum coherences, as these Hamiltonians induce changes in the coherence order of the magnetization state by one or two orders, respectively.

In Fig. 1c is shown a third variant, where a single- or double-quantum Hamiltonian is applied to directly excite multiple-quantum coherences from transverse magnetization (single-quantum coherences), generated by a 90° pulse. To reconvert the signal, the single- or double-quantum Hamiltonian is again applied to generate transverse magnetization. At the end of this sequence, two 90° pulses may be applied, between which Zeeman magnetization is selected, in order to combine the signals from the different pathways.

In all filtration experiments, best results will be obtained if the reconversion sequence carries out the reverse transformation to that carried out by the excitation sequence, thus ensuring that the signals from different molecules have the same phases. In the solution state this was achieved by using symmetric excitation and reconversion, as illustrated in Fig. 1a [7]. Under static conditions in the solid state, the problem was solved using so-called time-reversible sequences [16], whereby the average Hamiltonian during the excitation sequence can be reversed in sign for the reconversion sequence, so as to bring the signals from different parts of the sample with different dipolar couplings together with the same phase so that they add coherently. Under magic angle spinning (MAS) conditions, the problem is solved by the time periodicity of the spinning, necessitating only some form of synchronization between the sample rotation and either the timing or the phase of the reconversion sequence.

3.2. Selection rules

From the perspective of spin counting, the differences between the three schemes in Fig. 1 lie largely in the coherence orders which can be excited. More than one transition can occur in succession during a time period in which a particular Hamiltonian is acting. Hence, the overall changes which can occur in the coherence order and the number of spins involved in the magnetization state depend upon the cumulative effect of the possible changes. Selection rules have been derived [17–19] which illustrate the accessibility of particular magnetization states in spin systems of a particular size when particular multiple-quantum excitation schemes are used. Multiple-quantum excitation schemes may be categorized according to the initial state, the relative phases of certain pulses and the nature of the Hamiltonian acting during the excitation period (zero-, single- or double-quantum). Table 1 summarizes the accessibility of total coherence states for different combinations.

Figs. 2–4 show diagrammatically the coherence orders which can be exited in systems of spins $I = 1/2$ by the schemes given in Fig. 1. The vertical scale is the coherence order of the magnetization state, p, whilst the horizontal

Table 1
Selection rules for exciting total coherence in a system of spins $I = 1/2$, using different multiple-quantum excitation methods

Evolution Hamiltonian	Method	Selection rule
Zero-quantum	90° pulses in phase	z_g
	90° pulses $\pi/2$ out of phase	z_u
Single-quantum	Initial Zeeman magnetization	–
	Initial transverse magnetization	z
Double-quantum	Initial Zeeman magnetization	$2z_u$
	Initial transverse magnetization	z_u

z is any integer, z_g is any even integer and z_u is any odd integer. Note that the combination of longitudinal magnetization and a single-quantum Hamiltonian can generate a state with coherence one below total coherence for any number of spins.

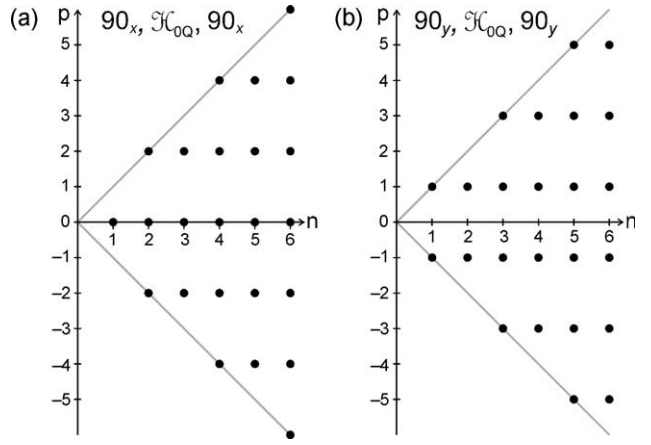

Fig. 2. Selection diagrams for spin counting experiments utilising a zero-quantum Hamiltonian, as in Fig. 1a. The circles mark those combinations of the coherence order, p, and the number of spins involved in the magnetization state, n, which are accessible. The grey lines mark the positions of states of total coherence, $n = \pm p$. (a) If the two 90° pulse have the same phase, all even coherence orders are accessible. (b) If there is a $\pi/2$ phase shift between the two 90° pulses, all odd coherence orders are accessible.

scale is the number of spins involved in the state, n. For a cluster of N spins $I = 1/2$, all accessible states with $n \leq N$ will be possible. The grey lines mark the bound $p = \pm n$, which is the position of states of total coherence.

Zero-quantum schemes, as in Fig. 1a, are restricted to observing only one parity of coherence orders. Which parity is observed depends upon the relative phases of the 90° pulses before and after the filtration point (shaded grey) to those at the beginning and end of the pulse sequence.

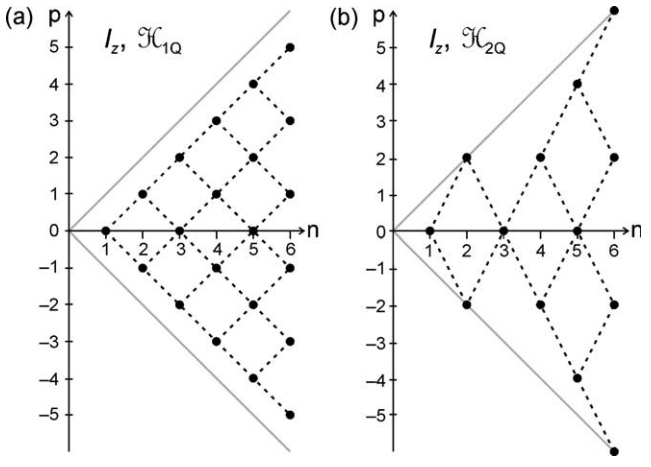

Fig. 3. Selection diagrams for spin counting experiments with an initial state of Zeeman magnetization, as in Fig. 1b. The circles mark those combinations of the coherence order, p, and the number of spins involved in the magnetization state, n, which are accessible. The dashed lines show the pathways by which the magnetization states are excited. The grey lines mark the positions of states of total coherence, $n = \pm p$. (a) A two-spin single-quantum Hamiltonian cannot generate total coherence but can excite all states with $N = \pm(p - 1)$. (b) A two-spin double-quantum Hamiltonian can only generate total coherence for values of $N = 2,6,10,\ldots$.

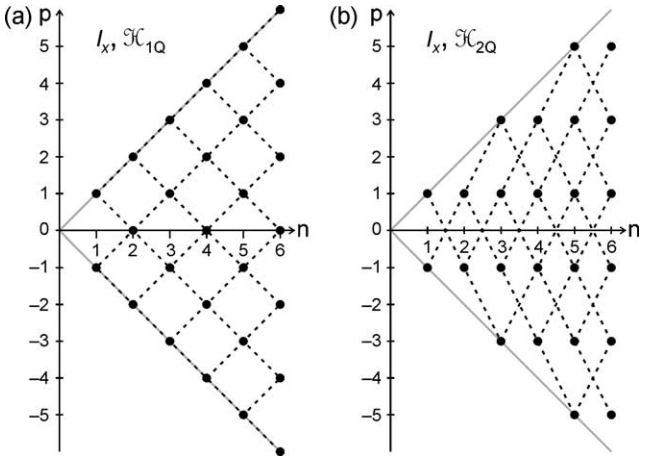

Fig. 4. Selection diagrams for spin counting experiments with an initial state of transverse magnetization, as in Fig. 1c. The circles mark those combinations of the coherence order, p, and the number of spins involved in the magnetization state, n, which are accessible. The dashed lines show the pathways by which the magnetization states are excited. The grey lines mark the positions of states of total coherence, $n = \pm p$. (a) A two-spin single-quantum Hamiltonian can excite all possible states of total coherence. (b) A two-spin double-quantum Hamiltonian can only excite states of total coherence with odd values of N.

A two-spin zero-quantum Hamiltonian will generate single-quantum states involving all possible combinations of spins in a cluster. The 90° pulse which follows will excite magnetization states with even coherence orders if it has the same phase as the first 90° pulse (Fig. 2a), whilst odd coherence orders will result if there is a $\pi/2$ shift in the phase between the two pulses (Fig. 2b). The phase difference between the third and fourth 90° pulses must fulfil the same condition. There is no additional restriction upon the accessibility of coherence orders caused by the number of interacting spins, in contrast to some of the cases described below.

Two-spin single-quantum Hamiltonian terms, such as those in Eq. (2), will induce changes of ± 1 in the coherence order, p, and of ± 1 in the number of spins involved in the state of magnetization, n, causing the parity of the sum $p + n$ to be constant. Hence, the availability of a given magnetization state depends upon the initial magnetization state. If a single-quantum mixing scheme is applied to a state of longitudinal magnetization (Fig. 3a), states for which the sum $p + n$ is odd will result, thus excluding any total magnetization state, for which $p + n$ is even. Such a mixing scheme can therefore only be used to assess the value $N - 1$ rather than N, allowing an estimate of the cluster size to be made [17]. However, an initial state of transverse magnetization (Fig. 4a) results in states for which $p + n$ is even, allowing all total coherence states to be accessible.

Two-spin double-quantum Hamiltonian terms, such as those in Eq. (3), induce changes of ± 2 in the coherence order and of ± 1 in the number of spins involved. This makes for more complicated selection rules. For an initial state of longitudinal magnetization (Fig. 3b), states are allowed with even values of p and values of n whose parities

do not match that of $p/2$. The combination of double-quantum mixing with an initial state of longitudinal magnetization is often called 'even-quantum spin counting', since all accessible states have even coherence order, but it should be noted that only every other even p total coherence state is accessible (i.e. $\pm p = N = 2, 6, 10, \ldots$). For an initial state of transverse magnetization (Fig. 4b), states are allowed with odd values of p and no restriction upon n, making the name 'odd-quantum spin counting' appropriate, since all states of total coherence with odd values of p can be excited.

3.3. Separating the multiple-quantum signals

The pulse schemes in Fig. 1 will all generate several different multiple-quantum magnetization states in between the excitation and reconversion sequences if a sufficient number of interacting spins are present. These can all contribute to the final signal and these contributions must therefore be separated. In each of the schemes shown in Fig. 1, the pulses before the point of filtration have a phase, ϕ, indicated by the hatching. Cycling of this phase can be used to separate out the different contributions to the final signal according to their coherence order at the filtration point.

This can be achieved in two ways. Standard phase cycling [20,21] can be used to select each coherence order in separate experiments, whilst a second method, introduced by Shykind et al. [22], enables the different signals to be acquired separately in a single experiment. Both methods rely upon the fact that the phase of the different contributions to the final signal is dependent upon the phase of the excitation sequence, ϕ, and the coherence order, p, between the excitation and reconversion sequences. The addition of signals acquired with varying values of ϕ and with the receiver phase set to $-p\phi$ for each signal acquisition will result in the constructive adding up of signals passing through coherence order p. Appropriate choice of a cycle for the phase ϕ can ensure that all other signals add up destructively, allowing only the signal from magnetization states with coherence order p to appear in the final spectrum.

Alternatively, the phase ϕ can be incremented between successive elements of a two-dimensional experiment. Successive points in the indirect dimension will be modulated by this phase, such that the signal, s, which has passed through coherence order p will be given by

$$s(p, \phi) = \exp\{-\mathrm{i}\phi p\} s(p, 0). \tag{4}$$

Fourier transformation in the ϕ dimension produces a spectrum with peaks at the values of p. The signal generated by such a method, as shown in Fig. 5a, is periodic over 2π radians. This signal is then processed in two steps. First, the signal is concatenated with itself to form a longer, repetitious signal (Fig. 5b). This is then Fourier transformed

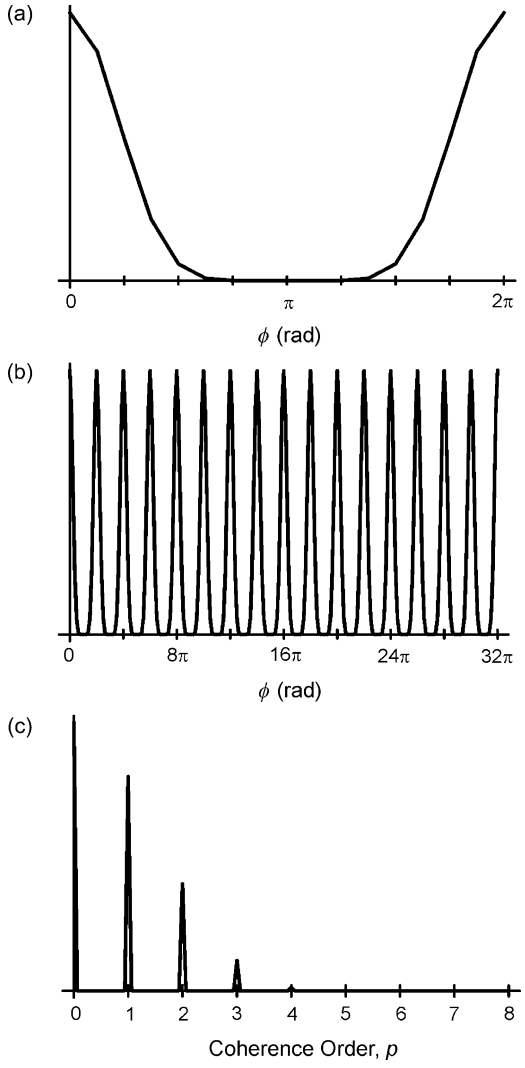

Fig. 5. (a) Simulated signal from a phase incremented spin counting experiment on a system of four interacting spins $I = 1/2$. (b) The signal from (a) repeated 16 times. (c) The Fourier transform of (b), showing the signal from $p = 0$ to 4.

to give the final spectrum (Fig. 5c) which is composed of delta-function lineshapes. Alternatively, the concatenated data may be apodized before Fourier transformation to give Lorentzian lineshapes. The amount by which ϕ is incremented, $\Delta\phi$, determines the spectral width and, therefore, the highest value of p which may be measured. This is given by

$$p_{\max} = \pi/\Delta\phi. \tag{5}$$

For the simulated data shown in Fig. 5a, the increment in ϕ is $\pi/8$, resulting in a value of eight for $p_{\max}$, as shown in Fig. 5c. The spectrum consists of lines whose intensity is proportional to the integral of a spectrum selective for the corresponding coherence order.

3.4. Multiple-quantum methods in the solution state

Spin counting was first carried out in solution-state NMR by Piantini et al. [1], with multiple-quantum filtered two-dimensional experiments revealing the *J*-coupling network between ^{1}H spins. The experiments used fall into the general class shown in Fig. 1a. The *J*-couplings between spins generate a zero-quantum Hamiltonian during a period of free precession. The chemical shifts may be refocused during the free precession periods with 180° pulses without refocusing the *J*-couplings. The effect of this zero-quantum Hamiltonian is to create anti-phase transverse magnetization which can be converted into various multiple-quantum coherences by a 90° pulse. As described above, the relative phases of the 90° pulses determines the parity of the coherence orders excited.

3.5. Multiple-quantum methods in the solid state

With the development of solid-state NMR techniques for multiple-quantum excitation, spin counting experiments could be carried out which revealed the dipolar coupling network between spins [2]. With the extension to solids undergoing MAS [3], spin counting was available for application to a wide range of problems [23].

Under static conditions, Pines and co-workers [2,13,24,25] developed several different pulse sequences for the generation of multiple-quantum coherences in solids. In particular, they addressed the problem of selective excitation, developing methods for generating average Hamiltonians containing only $\pm p$-quantum operators for a single value of p, leading, in particular, to the development of methods for generating double-quantum Hamiltonians. This work was supplemented by Suter et al. [18], who developed sequences for generating single-quantum Hamiltonians. These pulse sequences consist of combinations of groups of discrete r.f. pulses and delays to which supercycles are applied to generate the desired average Hamiltonian. A key property of these sequences is their so-called 'time reversibility' [25] described in Section 3.1.

These techniques, initially developed for ^{1}H NMR, were later modified for application to ^{13}C NMR [19,26], creating multiple-pulse sequences which take into account the chemical shift anisotropies which are much larger for ^{13}C than are the dipolar interactions. Whilst these methods are restricted to multiple-quantum filters on spins $I=1/2$, there are also techniques which have been developed for application to quadrupolar nuclei, specifically the $I=3/2$ ^{7}Li nucleus, under static conditions [15,27], for use in spin counting experiments. These made use of a magic echo, with a spin lock being applied during excitation (rotating-frame defocusing) followed by an echo sequence during detection (laboratory-frame refocusing). During the spin lock there are dipolar two-spin Hamiltonian terms and one-spin zero- and double-quantum terms arising from the quadrupolar coupling. Together, these two parts of the Hamiltonian ensure excitation of magnetization states involving several spins and all the possible coherence orders on each spin $I=3/2$ nucleus. The entire Hamiltonian, dipolar and quadrupolar, is reversed in sign and doubled in magnitude during the echo, ensuring refocusing of the signals.

Most spin counting studies in the solid state have been performed under static conditions rather than under MAS. This is not because of a lack of pulse schemes for generating the required Hamiltonians under MAS but because of the greater difficulty the schemes have in generating high orders of multiple-quantum coherence. MAS removes the effect of dipolar couplings and, hence, sequences are required which recouple this interaction. Recoupling may be achieved by introducing a second modulation to the spins, in addition to the spinning, which is synchronized with the spinning. In most cases, this second modulation is a radiofrequency pulse, giving rise to r.f. driven dipolar recoupling techniques. A second alternative is rotational resonance, where the matching of the isotropic chemical shift difference to the MAS frequency induces dipolar recoupling.

For spin $I=1/2$ nuclei, many multiple-quantum excitation sequences are available for generating zero- and double-quantum Hamiltonians using r.f. driven dipolar recoupling. The first were double-quantum dipolar recoupling schemes proposed by Meier and Earl [3]. These are sequences of discrete r.f. pulses and delays modified from the earlier, static sequences. Other dipolar recoupling sequences followed, including schemes built from discrete r.f. pulses applied at certain time points during the rotor period, such as RFDR [28] (which generates a zero-quantum Hamiltonian), and schemes with continuous r.f. irradiation whose phase is varied in a manner in synchrony with the sample rotation, such as C7 [29] (which generates a double-quantum Hamiltonian). Reviews covering this topic include Refs. [30–32].

Of particular note are dipolar recoupling sequences (such as C7) based upon the symmetry principles developed by Levitt and co-workers [29,30]. These allow the generation of many different average Hamiltonians, including zero-, single- and double-quantum dipolar Hamiltonians, with applicability to spin counting, in particular for conditions of fast MAS [33]. Additionally, Oyler and Tycko [34] have shown that the methods designed for the static case may be employed under MAS using the fpRFDR recoupling sequence [35] in place of periods of free precession. The recent development of three-spin triple-quantum recoupling schemes [14] carries with it the promise of further advances in solid-state multiple-quantum excitation methods.

3.6. Other methods for spin counting

Most magnetization states do not have a coherence order which is equal to the number of spins involved in the state. However, any magnetization state in which several spins are involved could, in principle, be used as indication for

the presence of spin clusters. By considering the coherence order of a state relative to the x- or y-quantization axis ($p^{(x)}$, $p^{(y)}$), rather than to the z-quantization axis (simply termed p), as is normally the case, other magnetization states can be exploited for the purpose of spin counting [9,36]. Of particular importance in this context are states of dipolar order, such as $I_z^{(i)}I_z^{(j)}$, $I_z^{(i)}I_z^{(y)}I_z^{(k)}$, etc. also known as multiple-spin order.

Under both static and MAS conditions, dipolar echoes [37] can be used for spin counting. The applications which have been performed [9] have been heteronuclear methods (see also below) where the number of spins of one species coupling to an individual spin of another species is measured. However, the dipolar echo itself is carried out on a single nuclear species. During a dephasing period, multiple-spin magnetization states develop in clusters of interacting spins. In a refocusing period the effect of the homonuclear dipolar interactions is reversed, leading to the echo. Between the two time periods is a pulse whose flip angle, χ, is varied. This causes modulation of the signals by a factor $\exp(i\chi p^{(y)})$. Fourier transformation with respect to χ results in a spectrum composed of peaks representing the efficiency of excitation and detection of each coherence order $p^{(y)}$, analogously to the method described in Section 3.3. As with the zero-quantum excitation schemes described earlier, exclusively odd or exclusively even values of $p^{(y)}$ are generated, dependent upon the relative phases of certain pulses.

Under static conditions, the Jeener–Broekaert [38] and ADRF/ARRF [39] sequences have been implemented on single crystals to generate dipolar order [36]. These methods, developed for the solution state, make use of the fact that in a static single crystal, the dipolar couplings to chemically identical nuclei are equal and constant and can therefore be utilised in the same manner as J-couplings. In these experiments, the coherence orders relative to both the z- and x-quantization axes can be encoded by the variation of two phases in the pulse sequence.

3.7. Heteronuclear methods

Three methods have been developed for heteronuclear spin counting, i.e. the counting of one species of nuclei which are coupled to a particular nucleus of a different species. The first was the dipolar echo method mentioned above. This was performed on ^{1}H and ^{13}C nuclei. Before the dipolar echo is performed, two cross-polarizations are carried out, the second with short duration, preparing a state in which only ^{1}H nuclei close to a ^{13}C nucleus are polarized. After the dipolar echo, a short cross-polarization is again performed to transfer signal to the closest ^{13}C nuclei, enabling the measurement of the number of ^{1}H nuclei near a particular ^{13}C nucleus.

In the second method [40], a variant of the spin echo double resonance (SEDOR) experiment was used. The original SEDOR experiment [41] allowed for the presence of a second nuclear spin species to be identified. A spin echo ($90°-\tau$ to $180°-\tau$) is performed on one nuclear species with and without a pulse applied to a second nuclear species at the same time as the 180° pulse. If the two nuclear species are interacting with one another, the additional pulse will cause the refocusing of the heteronuclear interaction, increasing the magnitude of the echo signal. The variant of the SEDOR experiment allowed the number of the second spin species to be measured, by varying the flip angle of the pulse applied to these spins. This modulates the echo amplitude in a manner dependent upon the number of spins, allowing this number to be measured by comparison to a theoretical model.

In a third approach [42], the same kind of information is obtained by using REDOR. Magnetization is transferred from one nuclear species into states of multiple-quantum coherences on a second, the coherence order being a measure of the number of spins as it is for most homonuclear spin counting experiments.

4. Interpreting the result

4.1. The problem

One might consider that the result of a count is simple to interpret, perhaps with allowance for any margins of error. Unfortunately, spin counting by NMR has a weakness which can necessitate, at best, careful consideration or, at worst, a complicated analysis to understand the result. The weakness of the technique is that the maximum coherence order observed in a spin counting experiment only sets a minimum bound on the number of spins present. The simplest interpretation is therefore to take this minimum bound as the number of spins present [17] but this carries with it an unknown upper error margin.

When seeking to establish the number of molecules forming a cluster, particularly when studying the distribution of molecules which each contain several of the spins being counted, an approximate count resulting from the maximum coherence order detected can suffice. One example was a study of hexamethylbenzene in NaY zeolite [43]. Since hexamethylbenzene contains 18 H atoms, it was concluded that a count of 16 H atoms was sufficient evidence to exclude the loading of cavities in NaY with more than one hexamethylbenzene molecule.

The principle cause of the problem is the fact that higher quantum coherences are increasingly difficult to excite. There are several reasons for this. First, higher coherence orders require longer excitation times, leading to relaxation becoming more significant. Second, the excitation efficiencies for higher coherence orders are often worse than for lower orders. Third, the number of magnetization states decreases with increasing coherence order. Consideration of this third factor alone has led to a method for interpreting spin counting results by fitting the signal intensities from

the different coherence orders to statistical models. Although doubt has been cast on the validity of these models [44,45], their wide use [2,9,15,27,33,46–60] necessitates a discussion in this review.

4.2. Statistical models

The number of p-quantum states in a spin system can be determined by combinatorial theory. For example, for a cluster of N spins $I=1/2$, the distribution is binomial:

$$Z(p) = \begin{pmatrix} 2N \\ N-p \end{pmatrix} \tag{6}$$

where $Z(p)$ is the number of p-quantum states. If it is assumed that the excitation efficiency of all individual magnetization states is equal, expressions such as Eq. (6) also define the distribution of the signal intensities from the different coherence orders, $\mathcal{I}(p)$, since $\mathcal{I}(p) \propto Z(p)$ under such conditions. This assumption may be valid if a random walk model [2] is applied and differential relaxation of the magnetization states is ignored. The random walk model was proposed to be applicable when multiple-quantum coherences are directly excited by a single- or double-quantum Hamiltonian which is applied for a period more than three or four dipolar correlation times.

For a cluster of spins I and for large values of N and small values of p, the distributions of states may be approximated to a Gaussian distribution [2,15]. With the assumption that $\mathcal{I}(p) \propto Z(p)$, this results in

$$\mathcal{I}(p) \propto \exp\left\{-\frac{p^2}{(4I-1)N}\right\}. \tag{7}$$

Thus, a plot of $\ln\{\mathcal{I}(p)\}$ against p^2 should be linear with a gradient equal to $-((4I-1)N)^{-1}$, giving an estimate of N, the number of interacting spins. For spin $I=1/2$, this simplifies to

$$\mathcal{I}(p) \propto \exp\left\{-\frac{p^2}{N}\right\}, \tag{8}$$

resulting in an expected gradient of $-N^{-1}$ for a plot of $\ln\{\mathcal{I}(p)\}$ against p^2. Commonly, the value of N derived from such a fit is plotted against excitation time, with a levelling off of N at long excitation times taken as a measure of the complete cluster size.

More complex models have also been used, such as one where the distribution of signal intensities is fitted to a two-Gaussian model (for $I=1/2$) [46,47,49],

$$\mathcal{I}(p) \propto m_c \exp\left\{-\frac{p^2}{N_c}\right\} + m_t \exp\left\{-\frac{p^2}{N_t}\right\}, \tag{9}$$

with $N_c < N_t$. The value N_c is interpreted as the cluster size and that of N_t as the total number of interacting spins, including interactions between clusters. In this way, signal intensity distributions in which small coherence orders have much higher efficiencies than a simple Gaussian distribution would predict are explained. Again, plots of N_c and N_t against excitation time are often given, with levelling off of the value of N_c indicating the cluster size whilst N_t continues to increase. Cho et al. [61] have proposed a model based on a sum of many different terms representing clusters of differing sizes for their study of quasi-one-dimensional spin clusters.

A second approach to overcoming the failure of the simple Gaussian model has been to take into account the known dipolar couplings between the spins, as first proposed by Levy and Gleason [62]. This method can be applied to systems for which sufficient local structural information is already known and the goal is the elucidation of the large-scale structure, such as the determination of dimensionality. It has found particular use in the study of one-dimensional spin chains [58,63].

4.3. Non-statistical methods

Unfortunately, there can be significant deviation from the Gaussian distribution of signal intensities [44,45] in spin counting experiments. This is largely because the assumption upon which Gaussian fitting is based, that the excitation efficiency of all magnetization states is equal (i.e. $\mathcal{I}(p) \propto Z(p)$), is open to serious question. The spin dynamics of systems of coupled nuclei have been extensively studied and shown to not always conform to the statistical distributions predicted by the assumption $\mathcal{I}(p) \propto Z(p)$. It has been shown that significant deviations from Gaussian distributions are even observed in such 'model' systems as ^{1}H nuclei in adamantane. Lacelle et al. [45] warned of extracting quantitative data from a fit to these distributions and put forward a more complex procedure, involving a scaling analysis. However, they concluded that the 'sensible and cautious' approach could simply be to take the largest observable coherence order as indicative of the size of the spin system.

Another alternative for solving the problem is to carry out simulations of the system in question, with different clustering arrangements, and to compare these simulations to the distribution of intensities of the signals due to the different coherence orders in the spin counting experiment. Clearly, such a method can take into account (given sufficient simulation time) the exact nature of the experiment being performed but it obviously requires sufficient knowledge of the possible clustering arrangements to be available in order to provide a reliable result. Such a case is that of amyloid fibrils [34,64], where a good estimate may be made of the distance between the individual strands of the β-sheets (see Section 5.5).

One of the early developments in solution-state spin counting was spin filtering [7], designed to selectively observe total coherence states [6]. Here, the behaviour of a magnetization state during a spin echo was observed. The echo refocuses the chemical shifts but not the J-couplings. Hence, because a total coherence state does not evolve

under *J*-coupling, a lack of evolution indicates that the state is total coherence.

One of the most recent developments in spin counting [8] is the application of the same principle to solid-state spin counting under MAS, using the SC14 sequence [65] to excite multiple-quantum coherences and the $SR4_4^1$ sequence [66] for zero-quantum recoupling. Zero-quantum recoupling is applied to the multiple-quantum coherences for a variable time to allow measurement of the decay curve. This is compared to a decay curve generated by applying a spin echo to the multiple-quantum coherences for the same times. For a state of total coherence, the two decay curves match, whilst for any other state, the zero-quantum recoupling experiment gives rise to much faster decay of the magnetization state than the spin echo. In this way, total coherence states may be identified without recourse to calculations or simulations.

5. Applications

Applications of spin counting have been made to a wide variety of inorganic and organic solids, together with liquid crystals and molecules in solution. They have provided useful information in areas ranging from catalysis to biomolecular structure elucidation. Whilst early applications concentrated on ^{1}H and ^{19}F nuclei, more recently, ^{13}C and ^{7}Li nuclei have become the focus of spin counting studies. Adamantane and similar solid organic compounds were examined by spin counting [2,46,56] and proved useful in establishing the technique. Coherence orders greater than 60 were observed and, using a simple Gaussian model, cluster sizes were estimated to be growing to more than 400 ^{1}H nuclei for the case of adamantane.

5.1. Distributions of atoms and small molecules

Spin counting has most frequently been used in the study of individual atoms and small molecules distributed on surfaces or throughout materials. By probing the arrangement of these atoms or molecules through their clustering, information can be obtained which is of great interest, particularly in the field of catalysis. One of the earliest solid-state applications of spin counting was to the adsorption of ethyne on platinum [67]. In this study, the ratio of double-quantum signal intensity to triple-quantum signal intensity was used to distinguish between different models for the nature of the adsorbed ethyne. Later studies examined hydrocarbon fragments on ruthenium catalysts [68,69]. The authors were able to put forward models for the deposition consistent with the maximum coherence order observed but they could not positively identify which fragments were present.

The distribution of hydrogen atoms in various materials has been investigated by spin counting. Two related studies were carried out on hydrogenated amorphous silicon [47] and silicon carbide [49]. A two-Gaussian model (Eq. (9)) was used to identify clusters of hydrogen atoms. Hydrogen in various silica based catalysts has also been studied [17,57], allowing the nature of the silica support to be investigated and an assessment of the density of hydrogen packing in the catalysts to be made. The deposition of fluorine on the surface of diamond powder particles has also been studied [54].

Bonded silica phases have been investigated using spin counting [51]. These consist of silane groups (SiR_3, R is an alkyl group) bound through an Si–O linkage to a silica surface (Fig. 6a). A Gaussian model was used to assess the size of the ^{1}H spin clusters in bound trimethyl silane (silica-O-$SiMe_3$). A cluster size of 10 ± 1 was claimed to be consistent with the nine hydrogen atoms in single trimethyl silane units, implying that these groups are well separated on the surface of the silica. In light of the deficiencies of the Gaussian model (Section 4.3), it is perhaps not unsurprising that an apparent over estimate was obtained.

Several studies have been performed on systems in which small molecules are dispersed in a matrix. Two kinds of matrices have been studied; polymers [53,55,59] and zeolites [43,52,60,70]. In polymers, studies have included ^{19}F spin counting on the photosensitive salts $[Ph_3S]^+[AsF_6]^-$ and $[Ph_3S]^+[SbF_6]^-$. A first study [53] demonstrated the use of ^{19}F spin counting for distinguishing between samples in which the salt was dispersed throughout the polymer and samples where the salt aggregates rather than disperses. In a second study [55], ^{19}F spin counting was used to measure the degree of dispersion of the salt in the polymer. The measurements were based on the relative intensities of the different multiple-quantum filtered signals, thus arriving at values for the degree of dispersion without recourse to a fitting procedure to estimate spin cluster sizes.

In zeolites, the loading of supercages in NaY with various organic molecules has been investigated [43,52,70]. In such studies, an approximate count of the number of clustering spins is often sufficient, as in the study of hexamethylbenzene in NaY zeolite [43] (see Section 4.1). A spin counting study of different loading levels of benzene in NaY [52] used the simple Gaussian model to analyse the data. For low loading levels, the results indicated the presence of different occupancies of benzene in the supercages whilst, at higher loading levels, more uniform

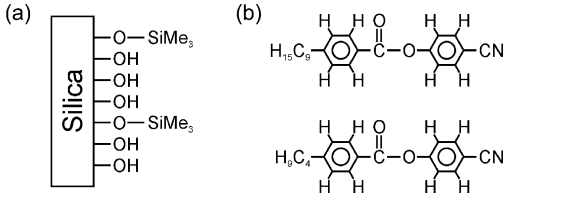

Fig. 6. (a) Trimethyl silane bound to silica, showing isolated trimethyl silane groups, as indicated by spin counting [51]. (b) The components of a liquid crystal on which Gerasimowicz et al. [50] carried out spin counting studies.

occupancy distributions were found, after allowances were made in the spin counting data for inter-supercage interactions between benzene molecules. The nature of chemical vapour deposition of Si_2H_6 [60] into the α-cages in NaY was also studied by ^1H spin counting. Fitting of the data to a Gaussian model gave a maximum ^1H cluster size of 38 ± 1, corresponding to the entrapment of seven disilane molecules per α-cage.

5.2. Liquid crystals

Liquid crystals were an early target of spin counting [46,50], partly because the motional properties of the molecules should average out intermolecular dipolar interactions whilst preserving intramolecular interactions, thus isolating the spins in individual molecules, making them a good model for isolated clusters. Indeed, simple Gaussian analysis of results on *p*-hexyl-*p*′-cyanobiphenyl indicated the formation of 21-spin clusters, corresponding to the number of ^1H nuclei in the individual molecules [46].

A second study on a two component liquid crystal [50] illustrated the possibility of distinguishing between separate groups of spins in the same molecule. The two components, shown in Fig. 6b, were combined in a 2:1 mixture. Both comprised of an alkyl group joined to a chain containing two aromatic rings, each of which contained two pairs of hydrogen atoms on adjacent carbons. Using a two Gaussian model with one cluster size set to two, a size was measured for the other cluster size of 13 ± 1, approximately the weighted average of the number of hydrogens in the two alkyl groups. The authors were unable to resolve separate contributions from the different alkyl chains.

5.3. Dimensionality and orientation

Although generally used either to measure the sizes of clusters or to distinguish between clusters and extended networks, spin counting has also been shown to be able to play a role in the study of samples known to contain extended networks of spins. The dimensionality of a network of spins has an effect upon the build-up rate of multiple-quantum coherences during a spin counting experiment. Levy et al. [62] showed that the build up of cluster size, as determined by fitting to a Gaussian distribution, is substantially different in two- and three-dimensional distributions, once the average dipolar interaction between the nuclei was taken into account. This was applied to study the distribution of hydrogen in chemically vapour deposited (CVD) diamond films.

One-dimensional chains have also been studied by spin counting [58,61,71]. In particular, apatites ($Ca_5X(PO_4)_3$, X = OH or F), which form chains with a hexagonal subunit containing seven H or F atoms, were studied. The effect of defects in the chains on the build up of multiple-quantum coherences was investigated. In addition, Fel'dman and Lacelle [63] carried out a detailed theoretical analysis of multiple-quantum dynamics in such systems, showing the deficiencies of the Gaussian model. In single crystals of CaF_2, ^{19}F spin counting has been shown to give distinct results dependent upon the orientation of the crystal with the magnetic field [72].

5.4. Quadrupolar nuclei

Spin counting has not been restricted to spin $I = 1/2$ nuclei. The spin $I = 3/2$ ^7Li nucleus has also been the focus of spin counting studies [15,27], with clusters of lithium in Li_xC_{60} being studied. In addition to using a distinct method for multiple-quantum filtration to those used for spin $I = 1/2$ (see Section 3.5), these studies also need a different method for analysing their results, since the coherence order in such systems is limited not to $\pm N$, where N is the number of spins, but to $\pm 3N$. A Gaussian distribution was used to interpret the results, applying Eq. (7) with $I = 3/2$:

$$\mathcal{I}(p) \propto Z(p) \propto \exp\left\{-\frac{p^2}{5N}\right\}. \tag{10}$$

The study found Li clusters smaller than were expected from stoichiometry. Two possible explanations were discussed; structural disorder or a failure of the statistical model, although the authors found no clear evidence of deviations from their model.

5.5. Amyloid fibrils

The application of spin counting to biomolecular solid-state NMR has been initiated by Tycko and co-workers, in studies of amyloid fibrils [34,64,73,74]. In particular, spin counting has been used to study the organization of the protein strands within the β-sheets which form the core of the fibrils, where a key question is whether the arrangement of consecutive strands is parallel, anti-parallel or some intermediate case, as shown in Fig. 7. The experiments have been performed on fibrils formed from the full length protein, $A\beta_{1-40}$ [73], and from a fragment of the protein,

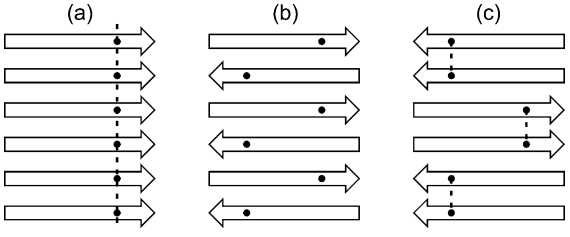

Fig. 7. Three possible arrangements of protein strands in the β-sheet core of an amyloid fibril. The arrows represent the direction of each protein strand. These are arranged (a) parallel, (b) anti-parallel and (c) one possible intermediate case, dimeric. The circles represent the positions of a ^{13}C label at a single site in the protein. The dashed lines represent the interactions between those ^{13}C nuclei in close proximity. Spin counting on $A\beta_{1-40}$ [73] indicated a parallel arrangement (a), whilst this arrangement was excluded for $A\beta_{16-22}$ [64].

$A\beta_{16-22}$ [64]. In both cases, the proteins contained specific ^{13}C labels.

In the study of fibrils formed by the full-length β-amyloid fibril, four-quantum coherences were observed from samples which contained a single ^{13}C label at the methyl position in one alanine residue. This information is strongly suggestive of a parallel arrangement of consecutive strands in the β-sheet (Fig. 7a), where the labelled residues line up in the strands next to one another. This conclusion was backed up by comparison with simulations, based on the known inter-strand separation of 4.8 Å.

The study of the fibrils formed by $A\beta_{16-22}$, again prepared with a single ^{13}C label at the methyl position in one alanine residue, gave different results. No coherence orders greater than three were observed, immediately suggesting that a parallel arrangement of the strands was unlikely. Comparison with simulations was not able to positively identify the nature of the arrangement but the simulations were shown to be not inconsistent with an anti-parallel arrangement (Fig. 7b). Tycko and co-workers have since gone on to more detailed examinations of different fibril forming peptides [75], demonstrating the value of spin counting in providing important, fundamental structural information which can act as the initial step of a full structural study.

6. Future prospects

Spin counting experiments are not in themselves capable of providing detailed structural information. However, in combination with other information they are able to complete the picture whilst, in other situations, they can provide a starting point for more comprehensive studies. Viewed in this way, and taking into account the increasing number of methods for exciting and observing multiple-quantum coherences (particularly under MAS), spin counting can reasonably be expected to continue to play a small but significant role in NMR. Given the example of the recent work on amyloid fibrils, it is clear that the concept of spin counting can follow NMR in whatever new directions it takes.

Acknowledgements

The Alexander von Humboldt foundation is thanked for the award of a fellowship. The author would like to thank Dr Henrike Heise for her careful reading of the manuscript.

References

[1] U. Piantini, O.W. Sørensen, R.R. Ernst, J. Am. Chem. Soc. 104 (1982) 6800.
[2] J. Baum, M. Munowitz, A.N. Garroway, A. Pines, J. Chem. Phys. 83 (1985) 2015.
[3] B.H. Meier, W.L. Earl, J. Chem. Phys. 85 (1986) 4905.
[4] R.J. Smernik, J.M. Oades, Geoderma 96 (2000) 101.
[5] P. Conte, R. Spaccini, A. Piccolo, Prog. Nucl. Magn. Reson. Spectrosc. 44 (2004) 215.
[6] D.P. Weitekamp, J.R. Garbow, J.B. Murdoch, A. Pines, J. Am. Chem. Soc. 103 (1981) 3578.
[7] O.W. Sørensen, M.H. Levitt, R.R. Ernst, J. Magn. Reson. 55 (1983) 104.
[8] C.E. Hughes, J.S.a.d. Günne, M.H. Levitt, Chem. Phys. Chem. 4 (2003) 457.
[9] M. Tomaselli, S. Hediger, D. Suter, R.R. Ernst, J. Chem. Phys. 105 (1996) 10672.
[10] L. Braunschweiler, G. Bodenhausen, R.R. Ernst, Mol. Phys. 48 (1983) 535.
[11] M.H. Levitt, R.R. Ernst, J. Chem. Phys. 83 (1985) 3297.
[12] J. Boyd, C.M. Dobson, C. Redfield, FEBS Lett. 186 (1985) 35.
[13] W.S. Warren, D.P. Weitekamp, A. Pines, J. Chem. Phys. 73 (1980) 2084.
[14] M. Edén, Chem. Phys. Lett. 366 (2002) 469.
[15] M. Tomaselli, B.H. Meier, M. Riccò, T. Shiroka, A. Sartori, J. Chem. Phys. 115 (2001) 472.
[16] Y.-S. Yen, A. Pines, J. Chem. Phys. 78 (1983) 3579.
[17] B.C. Gerstein, M. Pruski, S.-J. Hwang, Anal. Chim. Acta 283 (1993) 1059.
[18] D. Suter, S.B. Liu, J. Baum, A. Pines, Chem. Phys. 114 (1987) 103.
[19] R. Tycko, J. Magn. Reson. 139 (1999) 302.
[20] A.D. Bain, J. Magn. Reson. 56 (1984) 418.
[21] G. Bodenhausen, H. Kogler, R.R. Ernst, J. Magn. Reson. 58 (1984) 370.
[22] D.N. Shykind, J. Baum, B.-B. Liu, A. Pines, J. Magn. Reson. 76 (1988) 149.
[23] B.C. Gerstein, in: D.M. Grant, R.K. Harris (Eds.), Encyclopedia of Nuclear Magnetic Resonance vol. 5, Wiley, Chichester, 1996, p. 3144.
[24] W.S. Warren, A. Pines, J. Chem. Phys. 74 (1981) 2808.
[25] Y.S. Yen, A. Pines, J. Chem. Phys. 78 (1983) 3579.
[26] O.N. Antzutkin, R. Tycko, J. Chem. Phys. 110 (1999) 2749.
[27] T. Shiroka, M. Riccò, F. Barbieri, E. Zannoni, M. Tomaselli, Phys. Solid State 44 (2002) 521.
[28] A.E. Bennett, J.H. Ok, R.G. Griffin, S. Vega, J. Chem. Phys. 96 (1992) 8624.
[29] Y.K. Lee, N.D. Kurur, M. Helmle, O.G. Johannessen, N.C. Nielsen, M.H. Levitt, Chem. Phys. Lett. 242 (1995) 304.
[30] M.H. Levitt, in: D.M. Grant, R.K. Harris (Eds.), Encyclopedia of Nuclear Magnetic Resonance vol. 9, Wiley, Chichester, 2002, p. 165.
[31] G.P. Drobny, J.R. Long, T. Karlsson, W. Shaw, J. Popham, N. Oyler, P. Bower, J. Stringer, D. Gregory, M. Mehta, P.S. Stayton, Annu. Rev. Phys. Chem. 54 (2003) 531.
[32] M. Baldus, Prog. Nucl. Magn. Reson. Spectrosc. 41 (2002) 1.
[33] H. Geen, R. Graf, A.S.D. Heindrichs, B.S. Hickman, I. Schnell, H.W. Spiess, J.J. Titman, J. Magn. Reson. 138 (1999) 167.
[34] N.A. Oyler, R. Tycko, J. Phys. Chem. B 106 (2002) 8382.
[35] Y. Ishii, J. Chem. Phys. 114 (2001) 8473.
[36] H. Cho, D.G. Cory, C. Ramanathan, J. Chem. Phys. 118 (2003) 3686.
[37] S. Zhang, B.H. Meier, R.R. Ernst, Phys. Rev. Lett. 69 (1992) 2149.
[38] J. Jeener, P. Broekaert, Phys. Rev. 157 (1967) 232.
[39] C.P. Schlicter, W.C. Holton, Phys. Rev. 122 (1961) 1701.
[40] T.S. Cull, J.M. Joers, T. Gullion, R.E. Norberg, M.S. Conradi, J. Magn. Reson. 133 (1998) 352.
[41] D.E. Kaplan, E.L. Hahn, J. Phys. Radium 19 (1958) 821.
[42] K. Saalwächter, H.W. Spiess, J. Chem. Phys. 114 (2001) 5707.
[43] R. Ryoo, S.B. Liu, L.C.D. Menorval, K. Takegoshi, B. Chmelka, M. Trecoske, A. Pines, J. Phys. Chem. 91 (1987) 6575.
[44] M. Munowitz, Mol. Phys. 71 (1990) 959.
[45] S. Lacelle, S.-J. Hwang, B.C. Gerstein, J. Chem. Phys. 99 (1993) 8407.
[46] J. Baum, A. Pines, J. Am. Chem. Soc. 108 (1986) 7447.

[47] J. Baum, K.K. Gleason, A. Pines, A.N. Garroway, J.A. Reimer, Phys. Rev. Lett. 56 (1986) 1377.
[48] M. Munowitz, A. Pines, M. Mehring, J. Chem. Phys. 86 (1987) 3172.
[49] M.A. Petrich, K.K. Gleason, J.A. Reimer, Phys. Rev. B 36 (1987) 9722.
[50] W.V. Gerasimowicz, A.N. Garroway, J.B. Miller, J. Am. Chem. Soc. 112 (1990) 3726.
[51] W.V. Gerasimowicz, A.N. Garroway, J.B. Miller, L.C. Sander, J. Phys. Chem. 96 (1992) 3658.
[52] J.G. Pearson, B.F. Chmelka, D.N. Shykind, A. Pines, J. Phys. Chem. 96 (1992) 8517.
[53] B.E. Scruggs, K.K. Gleason, Macromolecules 25 (1992) 1864.
[54] B.E. Scruggs, K.K. Gleason, J. Phys. Chem. 97 (1993) 9187.
[55] S.J. Limb, B.E. Scruggs, K.K. Gleason, Macromolecules 26 (1993) 3750.
[56] Y. Ba, W.S. Veeman, Solid State NMR 3 (1994) 249.
[57] S.-J. Hwang, D.O. Uner, T.S. King, M. Pruski, B.C. Gerstein, J. Phys. Chem. 99 (1995) 3697.
[58] G. Cho, J.P. Yesinowski, J. Phys. Chem. 100 (1996) 15716.
[59] G. Buntkowsky, E. Roessler, M. Taupitz, H.M. Vieth, J. Phys. Chem. A 101 (1997) 67.
[60] J. He, Y. Ba, C.I. Ratcliffe, J.A. Ripmeester, D.D. Klug, J.S. Tse, K.F. Preston, J. Am. Chem. Soc. 120 (1998) 10697.
[61] G. Cho, J.P. Yesinowski, Chem. Phys. Lett. 205 (1993) 1.
[62] D.H. Levy, K.K. Gleason, J. Phys. Chem. 96 (1992) 8125.
[63] E.B. Fel'dman, S. Lacelle, J. Chem. Phys. 107 (1997) 7067.
[64] J.J. Balbach, Y. Ishii, O.N. Antzutkin, R.D. Leapman, N.W. Rizzo, F. Dyda, J. Reed, R. Tycko, Biochemistry 39 (2000) 13748.
[65] A. Brinkmann, M. Edén, M.H. Levitt, J. Chem. Phys. 112 (2000) 8539.
[66] A. Brinkmann, J.S.a.d. Günne, M.H. Levitt, J. Magn. Reson. 156 (2002) 79.
[67] P.-K. Wang, C.P. Schlichter, J.H. Sinfelt, Phys. Rev. Lett. 53 (1984) 82.
[68] S.-J. Hwang, T.S. King, B.C. Gerstein, Catal Lett. 8 (1991) 367.
[69] S.-J. Hwang, B.C. Gerstein, Bull. Magn. Reson. 15 (1993) 211.
[70] S.B. Hong, H.M. Cho, M.E. Davis, J. Phys. Chem. 97 (1993) 1622.
[71] L.B. Moran, J.P. Yesinowski, Chem. Phys. Lett. 222 (1994) 363.
[72] D.A. Lathrop, E.S. Handy, K.K. Gleason, J. Magn. Reson. A 111 (1994) 161.
[73] O.N. Antzutkin, J.J. Balbach, R.D. Leapman, N.W. Rizzo, J. Reed, R. Tycko, Proc. Natl Acad. Sci. USA 97 (2000) 13045.
[74] R. Tycko, Prog. Nucl. Magn. Reson. Spectrosc. 42 (2003) 53.
[75] A.T. Petkova, G. Buntkowsky, F. Dyda, R.D. Leapman, W.-M. Yau, R. Tycko, J. Mol. Biol. 335 (2004) 247.